The Climatic Effects of Biomass Burning: Investigations with a Global Climate Model

Robert J. Oglesby, Purdue University, West Lafayette, IN, USA, Susan Marshall, UNC-Charlotte, Charlotte, NC, USA, John A. Taylor, Australian National University, Canberra, Australia

Abstract A global climate model, the NCAR CSM, has been used to evaluate direct, indirect, and transport effects of the smoke from biomass burning. Biomass smoke is most important over tropical landmasses, especially South America, Africa, Southeast Asia and Australia. Biomass smoke distributions were estimated via a seasonally-varying source function that produced monthly mean estimates of the flux of trace gases to the atmosphere which were then confirmed qualitatively using satellite observations. The direct effect was modeled by assuming new cloud fractions wherever biomass smoke occurred. A sensitivity study was conducted to determine the most appropriate way to add these new 'clouds'. An indirect effect on existing clouds was modeled by reducing the cloud optical depth (which increases reflectivity) when they coincided with biomass smoke. Advection of the smoke has been accomplished by adding it as a tracer in the NCAR CCM3 (the atmospheric component of CSM). Preliminary results yield surface temperature reductions of several degrees and heating of the mid-levels of the atmosphere in the vicinity of major smoke emissions.

1. INTRODUCTION

Biomass burning can occur either as a result of natural causes (e.g., lightning) or through the actions of humans. Deforestation practices in the tropics and sub-tropics play a large role in the global total of biomass burned. Forest fires in the northern hemisphere provide an additional source of smoke, and have been the basis of a number of observational studies. The smoke produced by biomass burning in the southern hemisphere may be a relatively significant source of atmospheric particles, as fossil fuel emissions are much lower than in the northern hemisphere.

The smoke plumes that result from biomass burning are obvious on visible wavelength satellite images, being nearly indistinguishable from low and mid-level clouds, but are virtually absent on infrared wavelength images. This is because the particulates strongly reflect short-wave (solar) radiation, but are largely transparent to infrared (terrestrial) radiation. Biomass burning smoke plumes should therefore have a clear net cooling effect on the local and regional climate system. It was found by Robock [1991] that the presence of smoke plumes from forest fires in North America produced observed surface temperatures 1° to 6°C cooler than forecast (which did not take into account the smoke plumes). It was found by Penner et al. [1991] and [1992] that the radiative effects of biomass smoke may approach that of a doubling of CO_2 (though of the opposite sign) in affected regions. This means that in these regions the smoke may locally mask the effects of increased greenhouse gases.

The biomass smoke should also produce an indirect effect on the radiative balance of the region in which they occur. The smoke particles are effective cloud condensation nuclei and can induce an overall increase in the number of cloud droplets and a decrease in cloud droplet size. This leads to an increase in cloud reflectivity that may be as large or larger than the direct effect [Penner et al. 1992]. This indirect effect, in particular, has received little previous attention.

In addition to its local occurrence, the biomass smoke can be advected, both horizontally and vertically, by the prevailing winds. Besides simply enlarging the region affected by the smoke, this advection also means that an impact over downwind ocean regions may be expected. The response over ocean is likely very different than that over land.

We have made a series of general circulation model (GCM) simulations with the National Center for Atmospheric Research Community Climate Model, version 3 (CCM3) in order to examine further the climatic consequences of biomass burning. We examine both the direct and indirect effects as well as the vertical and horizontal transport of smoke outside of the source region.

Table 1: Sensitivity runs

	smkmax	*cldmax*	*levels*
Level-1	6.e10	0.9	2-3
Level-2	6.e10	0.9	2-5
Level-3	6.e10	0.9	2-7
Smkmax-1	1.e11	0.9	2-5
Smkmax-2	1.e10	0.9	2-5
Smkmax-3	1.e09	0.9	2-5
Cldmax-1	1.e11	0.3	2-5
Cldmax-2	1.e11	0.5	2-5
Cldmax-3	1.e11	0.6	2-5
Cldmax-4	1.e11	0.7	2-5
Cldmax-5	1.e11	0.9	2-5

* Simulations Cldmax-5 and Smkmax-1 refer to the same simulation.

The monthly values of biomass smoke emission are assumed to represent mid-month values and are linearly interpolated within the GCM code to daily values. Our standard approach is to normalize the smoke amount linearly to the maximum value of smoke for each time step. That is,

$$smoke'(j,t) = smoke(j,t) / smkmax \qquad (1)$$

where *smoke'* is the normalized smoke amount for grid square j at time step t; *smoke* is the actual smoke concentration (in g/month); and *smkmax* is a value chosen to represent the maximum value of smoke concentration for any grid square globally for any time of year. The absolute maximum value in the 12 month climatology produced by Taylor and Zimmerman is 1.47e11 g/month (occurs in January) with a mean for all smoke values of 1.78e9 g/month. Based on this, we chose 1e11 g/month as our basic value for *smkmax*, but also did experiments in which we varied *smkmax* from 1.e11 to 1.e9 (see Table 1). The lower the value of *smkmax* the relatively higher the value of *smoke'*. In all simulations, *smoke'* is not allowed to exceed 1.0, for those cases where *smoke* > *smkmax*.

The key parameter that must be calculated using *smoke'* is the fractional cloud cover of the smoke from biomass burning. Cloud fraction denotes the fraction of a unit area of sky covered by a cloud. These are defined for each vertical level in the model, and then vertically aggregated via a random overlap approach to provide total fractional cloud cover, i.e., that which would be seen from the earth's surface. In the standard model formulation, stratus clouds at any level have a fractional cover of 0.90, while convective clouds have a fractional cover of 0.30. Satellite and other observations suggest that initially smoke clouds from biomass burning resemble convective clouds (i.e., tall and narrow) but over time as they are trapped in certain atmospheric layers and spread horizontally by the wind, they resemble more stratus clouds (which have limited vertical extent but come close to filling the sky horizontally).

Our initial 'best guess' was that biomass burning smoke was best represented by convective clouds (nominal fractional cover of 0.30). Furthermore, we assumed a linear scaling in which the newly-introduced smoke clouds had maximum values (as determined by the source function) set to 0.30 with other values then scaled according to *smoke'*,

$$f_{smoke} = smoke' \times cldmax. \qquad (2)$$

We also made a simulation assuming that the maximum biomass smoke case represented a stratus cloud with fractional cover of 0.90. Then we made simulations with intermediate values of 0.5, 0.6, and 0.7 (Table 1). Scaling was linear in every case but one, in which a log scaling was used (this had the effect of forcing most smoke cloud values close to the *cldmax* values and was deemed to give unphysical results and is not presented in these results).

At each level where the smoke clouds are assumed to occur, the biomass smoke cloud fraction is combined with the water vapor cloud fraction to produce a total grid cloud cover fraction,

$$f_{cld} = (1 - f_{H2Ocld}) \times f_{smoke} + f_{H2Ocld} \qquad (3)$$

where f_{cld} is the total (water vapor cloud plus biomass smoke) cloud fraction, f_{H2Ocld} is the water vapor cloud fraction and f_{smoke} is the biomass smoke cloud fraction. The biomass 'clouds' affect only the calculation of short wave radiation in the model.

From our sensitivity studies and from observational evidence, we found the most reasonable choice of the above parameters to be smoke clouds in levels 2-5 of the model, maximum smoke amount set at 1.e11 and a value of *cldmax* set at 0.6. Figure 2 shows smoke cloud fraction plotted against absolute smoke concentration, for a case with *smkmax* = 1e11 and *cldmax* = 0.6. The linear scaling ensures that all points fall on a line but note the distribution - many more points have a small concentration and hence smoke fraction than at the high end.

2. SOURCES OF BIOMASS SMOKE

We used a seasonally-varying source function, developed by Taylor and Zimmerman [1991], to estimate the spatial and temporal distribution and of biomass burning clouds. This source function has a horizontal resolution of 2.5° latitude by 2.5° longitude and produces monthly mean estimates of the flux of trace gases to the atmosphere. The seasonal distribution of the flux of trace gases (and hence particulates) to the atmosphere was then apportioned inversely with respect to the amount of precipitation. This leads to large fluxes during the dry season, dwindling to near zero during the wet season. The precipitation climatology of Shea [1986] was used, and the model results for the variations in the extent and seasonality of biomass burning have been confirmed qualitatively using satellite observations. Figure 1 shows the mean monthly occurrence of biomass smoke for the representative months of January and July; the darker the gray shading the relatively greater the smoke concentration. Note the emphasis on southern hemisphere land masses and the seasonal shift north in January and south in July.

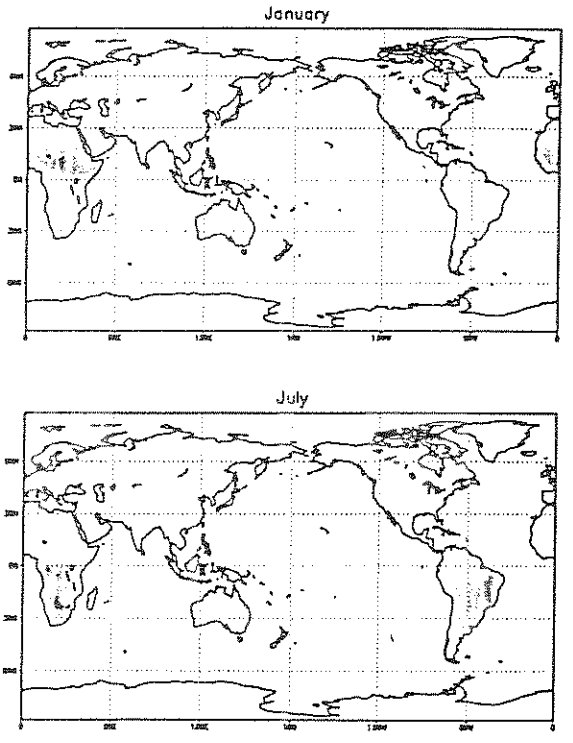

Figure 1: January (top) and July (bottom) biomass smoke concentration (in g/month). Intervals of 1.e10 g/month are shaded from 1.e10 to 9.e10.

3. MODELING APPROACH

All of the model simulations were made using the National Center for Atmospheric Research (NCAR) Community Climate Model, version 3 (CCM3). The CCM3 is described by Kiehl et al. [1996] and is global in domain and spectral in numerical formulation. That is, the linear horizontal terms are computed via Galerkin (spectral) techniques (utilizing the sphericity of the earth) while the horizontal nonlinear terms and the vertical terms are computed using finite differencing. The model has a triangular spectral truncation at wavenumber 42 (or T42) with a corresponding gridpoint resolution of 2.8° latitude by 2.8° longitude (conveniently close to that of the biomass smoke source function) and 18 vertical levels. Shortwave properties of clouds (crucial for both the direct and indirect effects) are parameterized following Slingo [1989]. A comprehensive, algorithmic description of the CCM3 routines is given in Kiehl et al. [1996].

3.1 Direct Effect: Cloud Cover Fraction

Adding biomass smoke 'clouds' into the model has three major parts: (1) determining the vertical levels in which the clouds occur; (2) scaling the cloud amount according to the relative amount of smoke present; and (3) varying the fraction of the sky covered by a smoke cloud. While some empirical evidence can be used as a qualitative guide, no theoretical framework exists with which to deduce these three properties. Therefore we conducted sensitivity tests in which we tuned these properties to yield a result that matched available observations.

Observations suggest that the vertical extent of the biomass smoke plumes is concentrated between 1-4 km above the surface [Andreae 1991]; this corresponds approximately to the lowest 5 layers in the model. We originally chose levels 2-5 (counting from the bottom) to implement the clouds (keeping the lowest level cloud-free as is consistent with 'real' clouds in the model). We also made simulations with clouds in levels (see Table 1) where we varied the top level of smoke cloud from level 3 in the model (approximately 900 mb or 1km) up to level 7 in the model (approximately 400 mb or 7 km).

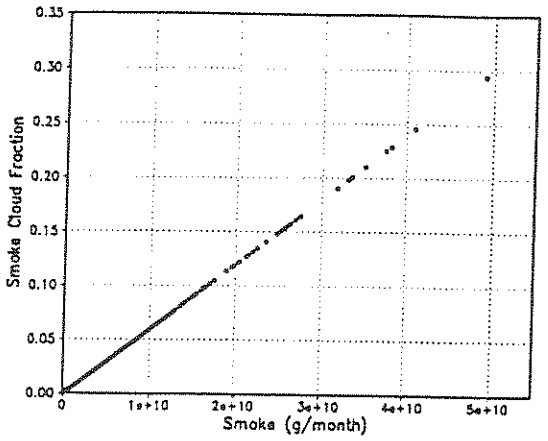

Figure 2: Smoke cloud fraction as determined from eqs.(1) and (2) using *smkmax* = 1.e11 and *cldmax* = 0.6.

3.2 Effect of Smoke Particles on Cloud Optical Properties

Aerosols emitted by the biomass burning are generally small (in the range from 0.1 to 0.2 mm), and highly effective as cloud condensation nuclei (Rogers et al. 1991). The result is a reduction of the effective (mass) droplet radius, thereby affecting the short-wave optical properties of the existing clouds (Woods et al. 1991). The second step of our three-pronged strategy involves investigating this indirect effect by reducing the mean cloud droplet radius of the existing clouds in regions of biomass burning (without adding new clouds as in step 1). In CCM3, the effective cloud liquid droplet radius generally varies between 5 and 10 microns (ice cloud droplets can be larger than 10 microns in some cases).

To address the indirect effect, we reduced the droplet radii by 50% whenever biomass burning smoke occurred as specified by our source function, and scaled the effect by the amount of smoke present (similar to the scaling for the direct effect). This produces clouds that are about 20% 'brighter' (i.e., have greater reflectivity) in the 10 micron case for a maximum smoke cloud.

3.3 Transport of Smoke Particles

Initial testing of smoke transport using the Australian National University Chemical Transport Model (ANU-CTM) shows the biomass smoke to remain fairly localized, the advection of smoke on the prevailing winds can extend the short-wave effects of the clouds downwind, and can also increase the mean vertical height of the smoke clouds. This model used European Common Market Medium-range Weather Forecasting (ECMWF) wind fields as a boundary condition, and was integrated through two simulated seasonal cycles. These results suggest that the smoke will disperse rapidly both vertically and horizontally, meaning the largest impact should be in and around those regions where the smoke occurs. Some of the smoke, however, will eventually be transported over the southern ocean, whose otherwise pristine atmosphere is likely to amplify the impacts of the smoke. To include this transport interactively within the model along with the direct and/or indirect effects, we are using the semi-Lagrangian tracer capability of the new NCAR CCM3 which allows for the model wind fields to move the smoke around as the model is run.

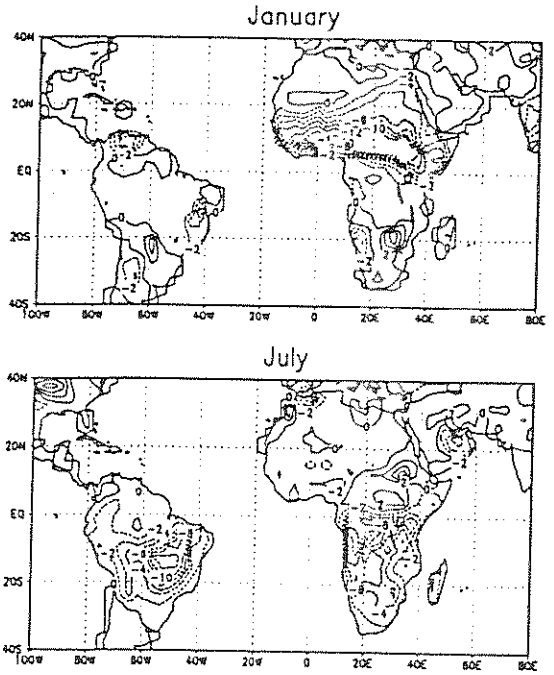

Figure 3: January (top) and July (bottom) surface temperature differences (Cldmax-3 minus control, in °C). Contour intervals of 2°C are shown, regions with differences exceeding 4° are shaded.

4. RESULTS AND DISCUSSION

4.1 Direct Effect: Adding Smoke Clouds

Although the qualitative effects of smoke clouds that result from biomass burning are well-known, we have no real idea how to quantify these effects. Based on the results of Robock [1991], we assumed we were targeting surface temperature reductions of 1-6°C in those regions of South America, Africa, and Australia strongly subject to biomass burning.

Figure 3 shows experiment minus control surface temperature differences for the 'best case' direct effect. Notice the coolings dominately over Africa in January and over both Africa and South America in July. Coolings range up to 12° C (although most regions have less than that) indicating that we have properly captured the effect of the new smoke clouds

Figure 4 shows surface temperature difference plotted against smoke concentration for those grid points with above a minimal amount of smoke. Note the generally negative linear trend (decreasing temperature with increasing smoke concentration) but with considerable scatter, which reflects model varaibility. Note also the clustering of points with small smoke concentrations and small temperature decreases, reflecting the distribution of smoke shown in Figure 2.

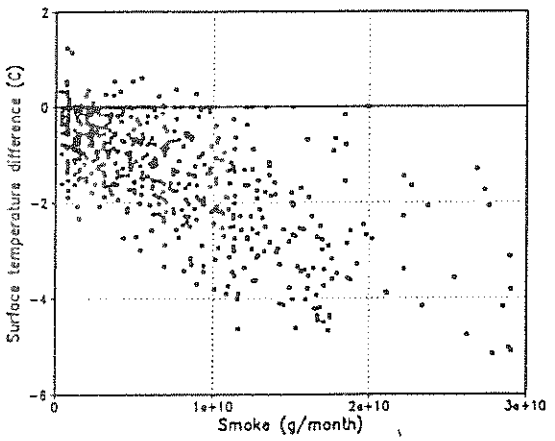

Figure 4: Surface temperature differences (Cldmax-3 minus control, in °C) compared to source smoke concentrations (g/month).

4.2 Indirect Effect: Decreasing Droplet Radius

The impact of smoke particles as a source of cloud condensation nuclei may be at least as significant as the direct effect of adding clouds in the simulations described above. Figure 5 shows the surface temperature response when only this indirect effect is imposed. Reducing the droplet size results in a brighter cloud (more reflectivity) and should decrease temperatures within and below the cloud relative to what would occur if the cloud were not enhanced. This effect is seen over regions of the African Sahel during January, with surface cooling exceeding 4°C in the areas of greatest smoke. An even larger effect is seen in July over southern Africa, with coolings exceeding 8°C. Temperature profiles (not shown) indicate these coolings to be confined to the layers within and below the clouds. The large effect over southern Africa is in a region with few clouds in the control but many clouds in the experiment. Thismsuggests a feedback occurs, creating more water clouds in the presence of smoke clouds than would otherwise happen, and hence essentially imposing both the direct and indirect effects in this region.

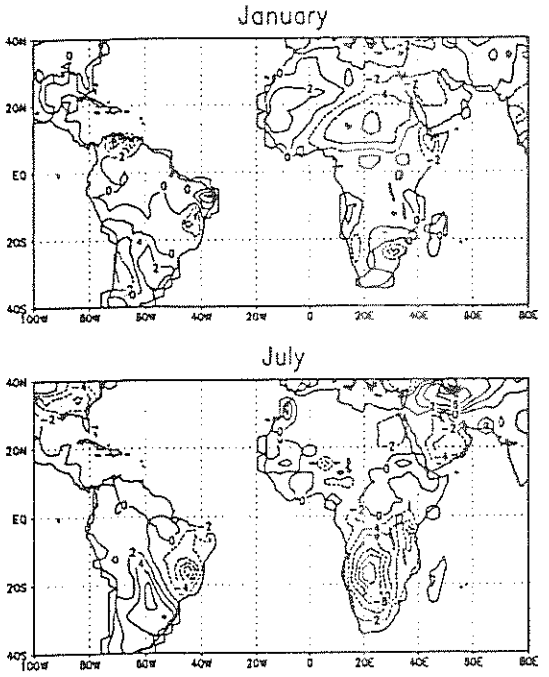

Figure 5: January (top) and July (bottom) surface temperature differences (Indirect effect minus control, in °C). Contour intervals of 2°C are shown.

5. SUMMARY AND FUTURE WORK

At this point of the project, we have been successful at simulating separately the direct and indirect effects. In reality, both effects will be taking place at the same time (but not necessarily at the same place as the indirect effect depends on the prior existence of a water vapor cloud while the direct effect does not). We made one preliminary simulation (not shown) combining both the direct and indirect effects. A key future goal is to successfully combine both direct and indirect effects.

Successful simulation of the direct and indirect effects, while extremely important, only addresses the effects of the biomass burning smoke in its source regions. In reality, a significant portion of the smoke may advect both vertically and horizontally (in work to date we account for vertical advection *in situ* but not vertical advection that occurs as the smoke is also advected horizontally). Off-line calculations suggest that the effects of the advected smoke are likely to be much smaller than those of the *in situ* effects, but nonetheless potentially significant. Future work will also be needed to address the full impact of he transport of smoke.

6. ACKNOWLEDGMENTS

This research has been supported in part by the US Department of Energy under grant DE-FG02-85ER14144 and a grant from the IBM Corp. Environmental Research Program, both to RJO, and by the US National Oceanic and Atmospheric Administration under grant NA36GP0396 to SM. Computational support was provided by the Scientific Computing Division of the US National Center for Atmospheric Research.

7. REFERENCES

Andreae, M.O., Biomass Burning: its history, use, and distribution and its impact on environmental quality and global climate. In: J.S. Levine (ed): *Global Biomass Burning: Atmospheric, Climatic, and Biospheric Implications*, MIT Press, Cambridge MA, pp. 3-21, 1991.

Kiehl, J.T., B. Boville, B. Briegleb, J. Hack, P. Rasch, and D. Williamson, Description of the NCAR Community Climate Model (CCM3). *NCAR Tech. Note, NCAR/TN-420+STR*, National Center for Atmospheric Research, Boulder, CO, 1996.

Penner, J.E., M.M. Bradley, C.C. Chaung, L.L. Edwards, and L.F. Radke, A numerical simulation of the aerosol-cloud interactions and atmospheric dynamics of the Hardiman Township, Ontario, Prescribed burn, in *Global Biomass Burning: Atmospheric, Climatic, and Biospheric Implications*, edited by J.S. Levine, pp. 420-426, MIT Press, Cambridge, 1991.

Penner, J.E., R.E. Dickinson, and C.A. O'Neill, Effects of aerosol from biomass burning on the global radiation budget. *Science, 256*, 1432-1433, 1992.

Robock, A., Surface cooling due to smoke from biomass burning, in *Global Biomass Burning: Atmospheric, Climatic, and Biospheric Implications*, edited by J.S. Levine, pp. 463-476, MIT Press, Cambridge, 1991.

Rogers, C.E., J.G. Hudson, B. Zielinska, R.L. Tanner, J. Hallett, and J.G. Watson, Cloud condensation nuclei from biomass burning, in *Global Biomass Burning: Atmospheric, Climatic, and Biospheric Implications*, edited by J.S. Levine, pp. 431-438, MIT Press, Cambridge, 1991.

Shea, D.J., Climatological Atlas: 1950-1979, *NCAR Tech. Note, NCAR/TN-269+STR*, National Center for Atmospheric Research, Boulder, CO, 1986.

Slingo, A., A GCM parameterization for the shortwave radiative properties of water clouds. *Journal of the Atmospheric Sciences, 46*, 1419-1427, 1989.

Taylor, J.A. and P.R. Zimmerman, Modeling trace gas emissions from biomass burning, in *Global Biomass Burning: Atmospheric, Climatic, and Biospheric Implications*, edited by J.S. Levine, pp. 345-350, MIT Press, Cambridge, 1991.

Woods, D.C., R.L. Chuan, W.R. Cofer III, and J.S. Levine, Aerosol characteristics in smoke plumes from a wetlands fire, in *Global Biomass Burning: Atmospheric, Climatic, and Biospheric Implications*, edited by J.S. Levine, pp. 240-244, MIT Press, Cambridge, 1991.